Swiss Journal of Geosciences (2018) 111:445–460
https://doi.org/10.1007/s00015-018-0315-6

Environmental changes and carbon cycle perturbations at the Triassic–Jurassic boundary in northern Switzerland

Nathan Looser[1] · Elke Schneebeli-Hermann[2] · Heinz Furrer[2] · Thomas M. Blattmann[1] · Stefano M. Bernasconi[1]

Received: 14 November 2017 / Accepted: 2 July 2018 / Published online: 26 July 2018

Abstract
The Triassic–Jurassic boundary is characterized by strong perturbations of the global carbon cycle, triggered by massive volcanic eruptions related to the onset of the Central Atlantic Magmatic Province. These perturbations are recorded by negative carbon isotope excursions (CIEs) which have been reported worldwide. In this study, Triassic–Jurassic boundary sections from the southern margin of the Central European Basin (CEB) located in northern Switzerland are analyzed for organic carbon and nitrogen isotopes in combination with particulate organic matter (POM) analyses. We reconstruct the evolution of the depositional environment from Late Triassic to Early Jurassic in northern Switzerland and show that observed negative shifts in $\delta^{13}C$ of the total organic carbon ($\delta^{13}C_{TOC}$) in the sediment are only subordinately influenced by varying organic matter (OM) composition and primarily reflect global changes in the carbon cycle. Based on palynology and the stratigraphic positions of isotopic shifts, the $\delta^{13}C_{TOC}$ record of the studied sections is correlated with the GSSP section at Kuhjoch (Tethyan realm) in Austria and with the St. Audrie's Bay section (CEB realm) in southwest England. We also show that in contrast to POM analyses the applicability of organic carbon/total nitrogen (OC/TN) atomic ratios and stable isotopes of total nitrogen ($\delta^{15}N_{TN}$) for detecting changes in source of OM is limited in marginal depositional environments with frequent changes in lithology and OM contents.

Keywords Triassic–Jurassic boundary · Northern Switzerland · Stable carbon and nitrogen isotope geochemistry · Sedimentology · Palynology · Chemostratigraphy

1 Introduction

The Triassic–Jurassic boundary biotic event is among the five largest mass extinction events of the Phanerozoic (Sepkoski 1996), involving turnovers in both marine and non-marine biota. This biotic crisis is associated with strong perturbations of the global carbon cycle which is recorded by negative carbon isotope excursions (CIEs) in carbonates and organic matter (OM) of latest Triassic and earliest Jurassic sediments (e.g. Pálfy et al. 2001; Hesselbo et al. 2002; Guex et al. 2004; Galli et al. 2005; Ruhl et al. 2009; Bacon et al. 2011; Črne et al. 2011; Bartolini et al. 2012; Lindström et al. 2012, 2017; Felber et al. 2015). These CIEs have been interpreted as inputs of isotopically light CO_2 into the atmosphere due to massive volcanic eruptions at the onset of the Central Atlantic Magmatic Province (CAMP) volcanism (Hesselbo et al. 2002). Positive feedback mechanisms such as the release of isotopically light seafloor methane hydrates triggered by induced global warming (Pálfy et al. 2001; Beerling and Berner 2002) may have intensified these global carbon cycle perturbations.

In marginal marine deposits, the relative proportion of marine and terrestrial OM in sediments can vary significantly. As such, a shift in the $\delta^{13}C$ record of the total organic carbon ($\delta^{13}C_{TOC}$) may represent a global change in the carbon cycle or merely a local variation in the

Editorial handling: S. Spezzaferri.

Electronic supplementary material The online version of this article (https://doi.org/10.1007/s00015-018-0315-6) contains supplementary material, which is available to authorized users.

✉ Nathan Looser
nathan.looser@erdw.ethz.ch

[1] Department of Earth Sciences, ETH Zurich, Sonneggstrasse 5, 8092 Zurich, Switzerland

[2] Institute and Museum of Paleontology, University of Zurich, Karl Schmid-Str. 4, 8006 Zurich, Switzerland

relative proportion of marine and terrestrial OM. Therefore, it is important to quantify their relative proportions in sediments. Modern terrestrial OM is about 7‰ lighter in $\delta^{13}C$ than marine OM (e.g. Killops and Killops 2005). $\delta^{13}C$ values for modern terrestrial C3 plants range from − 26 to − 30‰ and for modern marine phytoplankton from − 18 to − 22‰ (e.g. Cifuentes et al. 1996). However, marine OM was more depleted in ^{13}C during several periods of the Phanerozoic (e.g. Arthur et al. 1985). During these times, the difference in isotopic composition between terrestrial and marine OM was distinctly smaller or marine OM was even isotopically lighter than terrestrial OM. The reason for this is thought to be related to elevated aqueous CO_2 concentrations in the oceans during times of high atmospheric pCO_2 with higher CO_2 availability leading to greater isotope fractionation during photosynthesis (e.g. Kump and Arthur 1999). During latest Triassic and earliest Jurassic, marine OM had similar or 1–2‰ more negative $\delta^{13}C$ values than coeval terrestrial OM (Hayes et al. 1999; Hesselbo et al. 2002; Bartolini et al. 2012). Therefore, changes in the relative amounts of terrestrial and marine OM had smaller effects than in modern sediments. To isolate terrestrial from marine OM and evaluate its source-specific carbon isotopic composition, stable carbon isotopes of woody phytoclasts ($\delta^{13}C_{WP}$) have been successfully applied in Triassic–Jurassic boundary studies (Hesselbo et al. 2002; McElwain et al. 2009; Bacon et al. 2011). Alternatively, the source of preserved OM in the sediment can be assessed using particulate organic matter (POM) analyses, organic carbon/total nitrogen (OC/TN) atomic ratios or stable isotopes of total nitrogen ($\delta^{15}N_{TN}$). In contrast to POM analyses, OC/TN ratios and $\delta^{15}N_{TN}$ can be carried out at high resolution to detect possible rapid fluctuations in source of OM. However, OC/TN ratios and $\delta^{15}N_{TN}$ can be influenced by inorganic nitrogen fixed in clay minerals (Schubert and Calvert 2001) which hampers their applicability to record changes in the source of OM.

Despite the large number of studied sections, significant gaps remain in the reconstruction of global biogeochemical changes across the Triassic–Jurassic boundary, especially in marginal shallow-marine environments. Here, we present the first carbon isotope record of OM across the Triassic–Jurassic boundary from the Central European Basin (CEB) in northern Switzerland. We use particulate organic matter (POM) data and carbon isotopes of woody phytoclasts ($\delta^{13}C_{WP}$) to evaluate shifts in the bulk organic carbon isotope record. Also, we examine the applicability of OC/TN ratios and $\delta^{15}N_{TN}$ for detecting changes in OM sources by comparing them to POM data.

2 Geological overview

The studied sections were deposited at the southern margin of the CEB (Fig. 1a), a peri-Tethyan, epicontinental basin situated at paleolatitudes between 35 °N and 50 °N (Stampfli and Kozur 2006) which extended from northern Switzerland to southern Scandinavia and from eastern Great Britain to eastern Poland (Ziegler 1990). The CEB was separated from the Tethys by the Vindelician-Bohemian High in the south–east and by the Central Massif in the south–west. The only connection between the CEB and the Tethys was the Burgundy–Alemannic gate (Ziegler 1990) through which spatially limited marine ingressions from the Tethys influenced the depositional environment in the southern CEB (Fischer et al. 2012). In central and northern Europe, the CEB is characterized by discontinuous sedimentation across the Triassic–Jurassic boundary (e.g. Hallam 2001) whereas on the shelf of the western Tethys, sedimentation is more continuous as seen in the Northern Calcareous Alps (e.g. Ruhl et al. 2009). The succession of Rhaetian and Hettangian sediments in northern Switzerland is composed of the Gruhalde and Belchen Members (both Klettgau Formation) and the Schambelen and Beggingen Members (both Staffelegg Formation). More information regarding the general

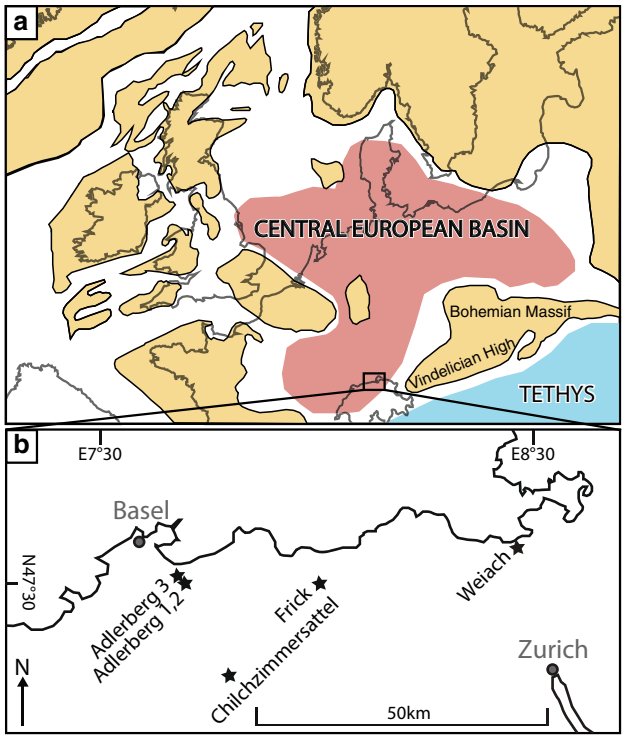

Fig. 1 **a** Paleogeographic map based on Ziegler (1990) and Stampfli and Kozur (2006). Modified from Schneebeli-Hermann et al. (2018). **b** Study area. Modified from Schneebeli-Hermann et al. (2018)

stratigraphy can be found in Schneebeli-Hermann et al. (2018) and references therein.

3 Study sites

For this study, four drill cores and two outcrops in northern Switzerland were analyzed (Fig. 1b). Three cores from the Adlerberg mountain south-east of Basel [Adlerberg 1 (core "34.R.3" in the borehole cadaster of canton Baselland, Swiss coordinates LV95: 2620027/1261176), Adlerberg 2 (core "34.R.8", coord.: 2620083/1261127), and Adlerberg 3 (core "41.R.117", coord.: 2618725/1262213)], one core from Weiach north of Zurich [core of the National Cooperative for the Disposal of Radioactive Waste (Nagra), coord.: 2676745/1268618, Matter et al. 1988], one outcrop in Frick in the canton Aargau (coord.: 2643000/1261900), and one outcrop at the Chilchzimmersattel north of the Belchen mountain in canton Baselland (type section of the Belchen Mb., coord.: 2627690/1246165, Jordan et al. 2016).

4 Methods

4.1 Stable C and N isotopes and C/N atomic ratios of bulk OM

The cores and outcrops were mostly sampled in a constant resolution of 2.5 or 5 cm. Sandstones, siltstones, clays, marls, and limestones were sampled avoiding fissures, fossils, nodules, and intraclasts. A total of 434 samples were finely ground and decarbonated with 3 M HCl for 24 h. The residue was repeatedly washed with deionized water, centrifuged, freeze-dried, and homogenized with a mortar and pestle. The samples were wrapped in tin capsules and total organic carbon (TOC) and total nitrogen (TN) contents and their carbon ($\delta^{13}C_{TOC}$) and nitrogen ($\delta^{15}N_{TN}$) isotope compositions were measured using a 1112 Flash EA connected to a Delta V IRMS (both Thermo Fisher Scientific, Bremen, Germany) at ETH Zurich. Isotope ratios are reported in the conventional δ-notation with respect to atmospheric N_2 (AIR) and VPDB (Vienna Pee Dee Belemnite) standards, respectively. The methods were calibrated with IAEA-N1 ($\delta^{15}N = +0.45‰$), IAEA-N2 ($\delta^{15}N = +20.41‰$), and IAEA-N3 ($\delta^{15}N = +4.72‰$) reference materials for nitrogen and NBS22 ($\delta^{13}C = -30.03‰$) and IAEA CH-6 ($\delta^{13}C = -10.46‰$) for carbon. Reproducibility of the measurements is better than $\pm$ 0.2‰ for both nitrogen and carbon.

4.2 Stable carbon isotope measurements of isolated woody phytoclasts

Woody phytoclasts were isolated by ultrasonication in deionized water and sieving through a 160 µm mesh. Woody phytoclasts were then extracted under a binocular, decarbonated for 96 h by HCl vapors, and neutralized for 72 h in the presence of hygroscopic NaOH. Several woody phytoclasts were weighted in tin capsules and measured as described above.

4.3 Carbonate and TOC content

For a total of 202 samples, total inorganic carbon (TIC) and total organic carbon (TOC) contents in weight percent were determined with a Coulometrics CM CO2 coulometer. For TIC measurements, the samples were dissolved in heated 2 M perchloric acid for 5 min. Total carbon (TC) content was determined by combustion at 950 °C. TOC was calculated as the difference between TC and TIC. TIC contents were converted to carbonate contents based on stoichiometry and atomic weights.

4.4 Particulate organic matter analyses

A total of 47 samples were cleaned, crushed, and 13–20 g were treated with concentrated HCl and HF (Traverse 2007). The residues were sieved through a 11 µm mesh. From the resulting strew mounts, a minimum of 300 particles was counted for the analysis of the particulate organic matter (POM) content.

5 Stratigraphy and sedimentology of the studied sections

The analyzed uppermost meters of the Gruhalde Mb. consist of greyish to greenish marly mudstones with TOC contents of $\sim$ 0.1% and constant carbonate contents of $\sim$ 20% (Figs. 2 and 3). Two horizons of matrix-supported conglomerates with poorly rounded dolomitic intraclasts of up to 2 cm in diameter are intercalated and in the Adlerberg 2 core, also a dolomitic layer occurs. Branchiopod crustaceans, fish scales, bone fragments, and a tooth of an archosaur reptile (Phytosauria, gen. et sp. indet.) as well as wood particles were observed. Fossils show little diversity and are scarce while fine-grained framboidal pyrite occurs throughout. Based on the occurrence of two palynomorphs, an Early Rhaetian age for the uppermost part of the Gruhalde Mb. is considered possible by Schneebeli-Hermann et al. (2018).

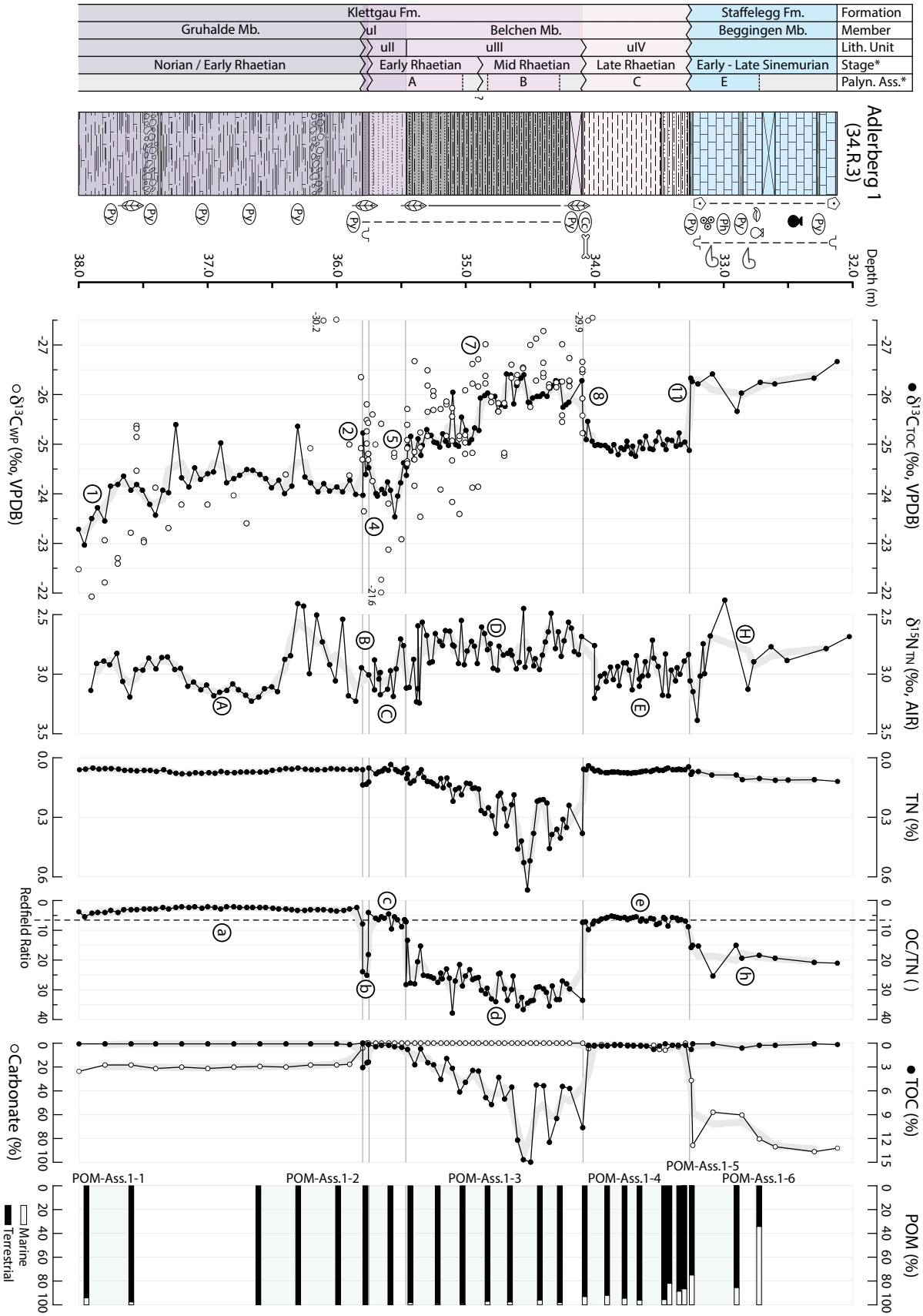
Klettgau Fm.
Staffelegg Fm.
Formation
Gruhalde Mb.
ul
Belchen Mb.
Beggingen Mb.
Member
ull
ulll
ulV
Lith. Unit
Norian / Early Rhaetian
Early Rhaetian
Mid Rhaetian
Late Rhaetian
Early - Late Sinemurian
Stage*
A
B
C
E
Palyn. Ass.*
Adlerberg 1 (34.R.3)
Depth (m)
δ13CTOC (‰, VPDB)
δ13CWP (‰, VPDB)
δ15NTN (‰, AIR)
TN (%)
OC/TN ( )
Redfield Ratio
TOC (%)
Carbonate (%)
POM (%)
Marine
Terrestrial
POM-Ass.1-1
POM-Ass.1-2
POM-Ass.1-3
POM-Ass.1-4
POM-Ass.1-5
POM-Ass.1-6

◀**Fig. 2** Stratigraphic column and results for the Adlerberg 1 core. Thick grey lines show three-point moving averages. Information about the palynological associations and stages are from Schneebeli-Hermann et al. (2018)

The following Belchen Mb. varies considerably in thickness between the four sections (Figs. 2, 3, and online resources 1 and 2). Nevertheless, in all sections it shows a continuous fining-upward sequence ranging from well-sorted, fine-grained sandstones at the base to claystones at the top. White mica and angular quartz grains, with the highest contents at the base, occur in great abundance in all sections except at the Chilchzimmersattel. TOC-rich parts contain abundant well-preserved brown and black wood and leaf fragments. Several bivalves and shark teeth were found at the Chilchzimmersattel (Jordan et al. 2016). Based on lithology and/or TOC content, the Belchen Mb. is here subdivided into the following four lithological units (Figs. 2, 3, and online resources 1 and 2):

Unit uI is composed of white mica-rich sandy siltstones or siltstones with angular quartz. It has a thickness of 5 cm in the Adlerberg 1 core and 115 cm in the Adlerberg 3 core. TOC contents reach almost 3% while carbonates are completely absent. Bioturbation occurs along the basal contact. In the Chilchzimmersattel outcrop, uI was not observed.

Unit uII shows a variable thickness ranging from 30 cm in the Adlerberg 1 core to at least 300 cm in the Adlerberg 2 core and ~ 250 cm in the Chilchzimmersattel outcrop where significant lateral changes in thickness within few meters indicate channel structures. It has distinctly lower TOC contents than uI. In the Adlerberg 2 core, well-sorted fine-grained quartz sandstones alternate with clay and sand-bearing siltstones. Asymmetric ripple marks in the quartz sandstone of the basal part as well as flaser bedding in the siltstones in the middle of uII are found and extensive bioturbation occurs almost throughout uII. Carbonate contents are very low with the exception of some carbonate-rich pebbles.

In unit uIII, the fining-upward continues gradually from sandy siltstones at the base to silty claystones at the top. The thickness is 135 cm in the Adlerberg 1 core, 180 cm in the Adlerberg 2 core, and 140 cm in the Chilchzimmersattel outcrop. It is characterized by high TOC of up to 15%. Centimeter-sized black and brown wood and leaf fragments are abundant. The entire uIII is laminated and carbonate-free except for diagenetic calcite nodules occurring directly below the contact to uIV. In contrast to the Adlerberg cores, extensive bioturbation is present throughout uIII at Chilchzimmersattel. At the contact between uIII and uIV of the Adlerberg 1 core, two dolomitic layers enriched in bone fragments and teeth were described by Lauber (1991), but are now missing from the core.

Unit uIV is composed of nodular grey and red claystones in the lower part followed by laminated siltstones and silty claystones with increasing white mica contents in the upper part. It is 85 cm thick in the Adlerberg 1 core and 35 cm in the Adlerberg 2 core. In the Adlerberg 1 core, uIV is completely preserved, while in the Adlerberg 2 core the upper part is missing and uIV is absent at the Chilchzimmersattel. This succession of claystones, siltstones and silty claystones shows a short sequence of coarsening-upward and subsequent fining-upward. TOC contents decrease to below 0.5% on average, while carbonate contents average 2%. No fossils or macroscopic phytoclasts were found within uIV.

Lithological units uI, uII, and the lower part of uIII containing the palynological association A are of Early Rhaetian age, the upper part of uIII containing the palynological association B is of Middle Rhaetian age, and uIV containing the association C is of Late Rhaetian age (see Schneebeli-Hermann et al. 2018 for description and correlation of the palynological associations), see Figs. 2, 3, and online resources 1 and 2.

The Schambelen Mb. with a thickness of 625 cm in the Weiach core and around 200 cm in the Frick outcrop can be divided into a lower part belonging to the upper part of the Planorbis zone and an upper part belonging to the Liasicus zone (Jordan 1983; Reisdorf et al. 2011). The lower part with a thickness of 85 cm in the Weiach core and 110 cm in the Frick outcrop consists of finely laminated pyrite-rich bituminous sandy to silty claystones with TOC contents of up to 6% in Frick and 4% in Weiach and low carbonate contents. The erosive contact to the underlying Gruhalde Mb. is sharp and without bioturbation. The upper part consists of silty claystones with less than 1% TOC and up to 15% carbonate and contains sand-rich layers. White mica and quartz are ubiquitous. With a thickness of 115 cm compared to 540 cm in Weiach the upper part of the Schambelen Mb. in Frick is considerably thinner, while the thickness of the lower part is similar. The occurrence of the palynological association W throughout the Schambelen Mb. in Weiach suggests a Hettangian age (Schneebeli-Hermann et al. 2018).

The Beggingen Mb. consists of tens of centimeters thick fossil-rich limestones with phosphorite nodules interrupted by few centimeters thick layers of dark marls containing pyrite. It is between 300 and 400 cm thick in all sections. Carbonate contents exceed 30% in the marly layers and 90% in the limestones, while TOC is lower than 1%. In the Adlerberg cores, the Schambelen Mb. is missing and the Beggingen Mb. unconformably overlies uIV of the Belchen Mb. A rich fauna including the ammonites *Arnioceras* sp. and *Paracoroniceras* sp., the bivalves *Gryphaea arcuata*,

Cardinia sp., *Plagiostoma* sp., *Chlamys* sp., and *Pinna* sp., the brachiopods *Spiriferina walcotti*, *Piarorhynchia juvensis*, and *Zeilleria vicinalis* as well as echinoderms, foraminifers, and bryozoans is present. The lowermost limestones contain iron ooids, peloids, and bioclasts in a sparitic cement. Above, the limestones change toward packstones and biomicrites. The ammonites *Arnioceras* sp. and *Paracoroniceras* sp. document an Early Sinemurian

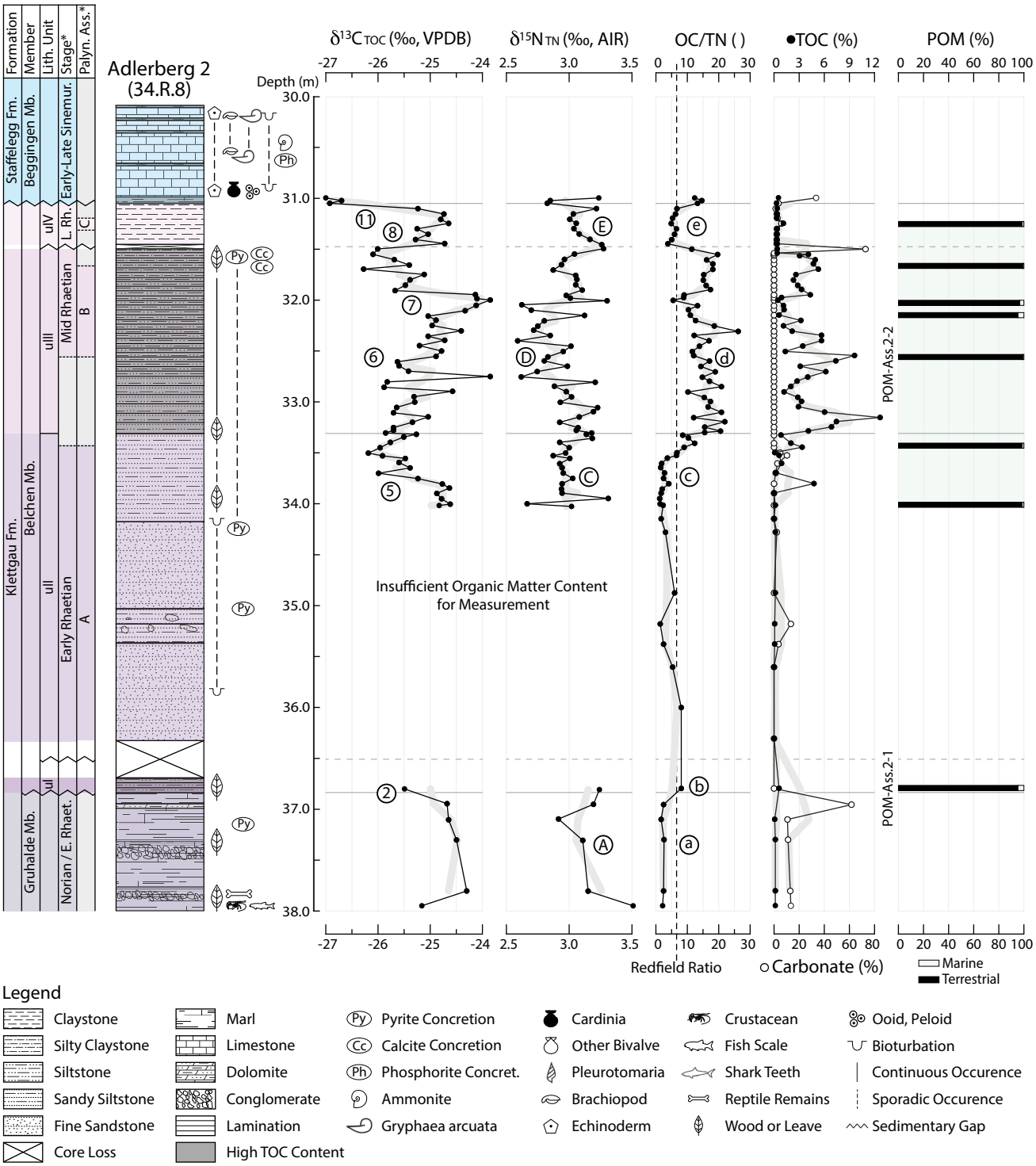

Fig. 3 Stratigraphic column and results for the Adlerberg 2 core. Thick grey lines show three-point moving averages. Information about the palynological associations and stages are from Schneebeli-Hermann et al. (2018)

age for the base of the Beggingen Mb. in the Adlerberg cores and in the Chilchzimmersattel outcrop, in good agreement with the palynological association D indicating a Hettangian to Sinemurian age (Schneebeli-Hermann et al. 2018). In the Frick outcrop, the more complete Beggingen Mb. has a Late Hettangian to Late Sinemurian age (Reisdorf et al. 2011).

6 Geochemistry

6.1 Carbon isotope stratigraphy

A total of 11 major shifts in the organic carbon isotope record were observed (Figs. 2, 3, 4, and online resources 1, 2, and 3). The $\delta^{13}C_{TOC}$ values vary between − 23 and − 29.5‰ and the $\delta^{13}C_{WP}$ between − 21 and − 30‰. An overall trend from higher $\delta^{13}C_{TOC}$ values in Early Rhaetian to lower values in Hettangian sediments is evident. All sections contain sedimentary gaps so that, in order to obtain a more complete carbon isotope record, the Adlerberg 1, 2, and Weiach cores were combined in a composite stratigraphic column (Fig. 5). The first shift (**1**) with a gradual decrease of − 1.5‰ occurs completely within the uppermost part of the Gruhalde Mb. and can be seen in the Adlerberg 1 core (Fig. 2). The abrupt second shift (**2**) of up to − 1.2‰ is found along the discontinuous contact between the top of the Gruhalde Mb. and uI of the Belchen Mb. and can be seen in the Adlerberg 1 and 2 cores (Figs. 2, 3). In the Adlerberg 3 core (online resource 1), uI seems to be present but without the negative shift (**2**) at the boundary between the Gruhalde Mb. and the Belchen Mb. Instead, a

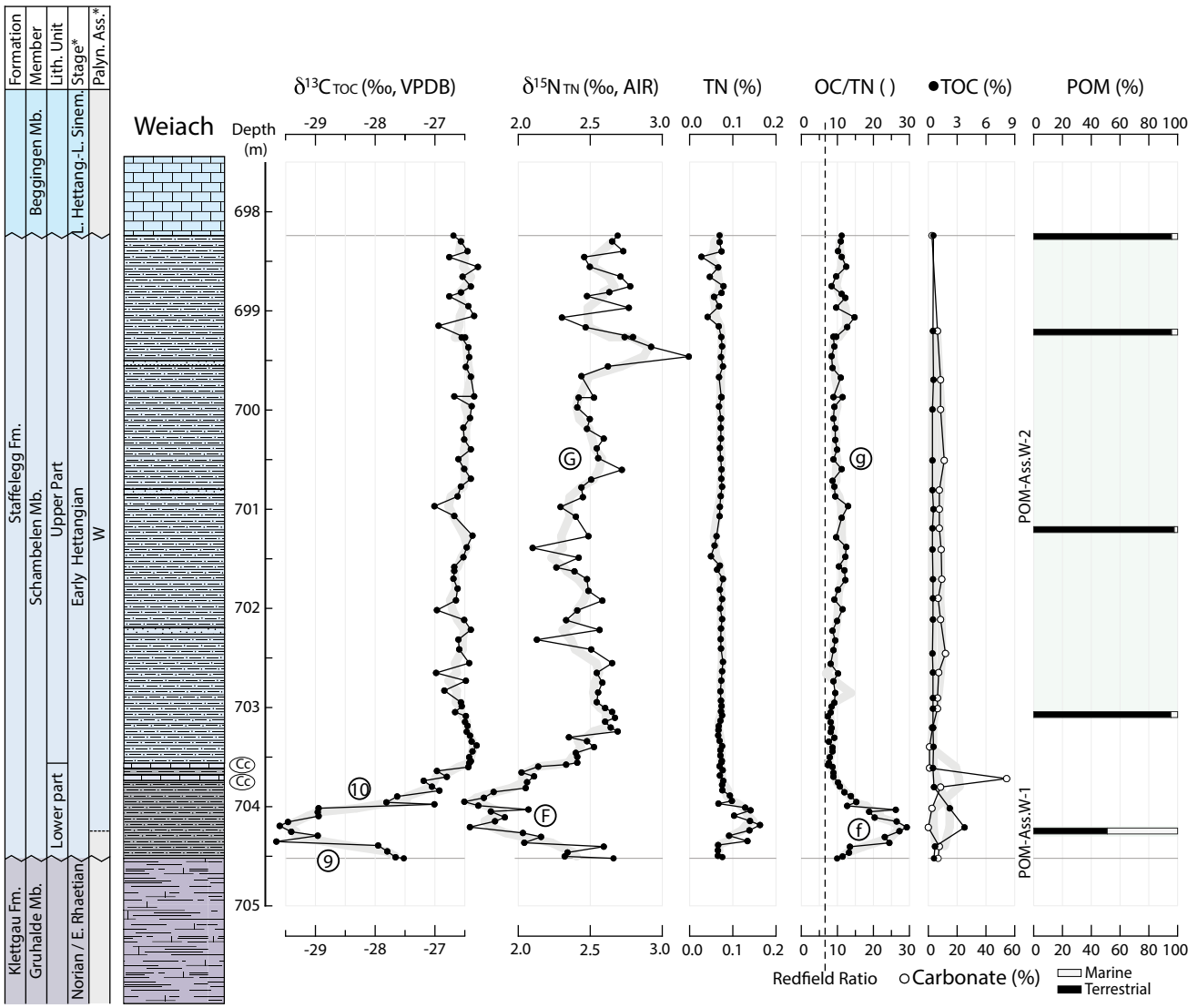

Fig. 4 Stratigraphic column and results for the Weiach core. Thick grey lines show three-point moving averages. Information about the palynological associations and stages are from Schneebeli-Hermann et al. (2018)

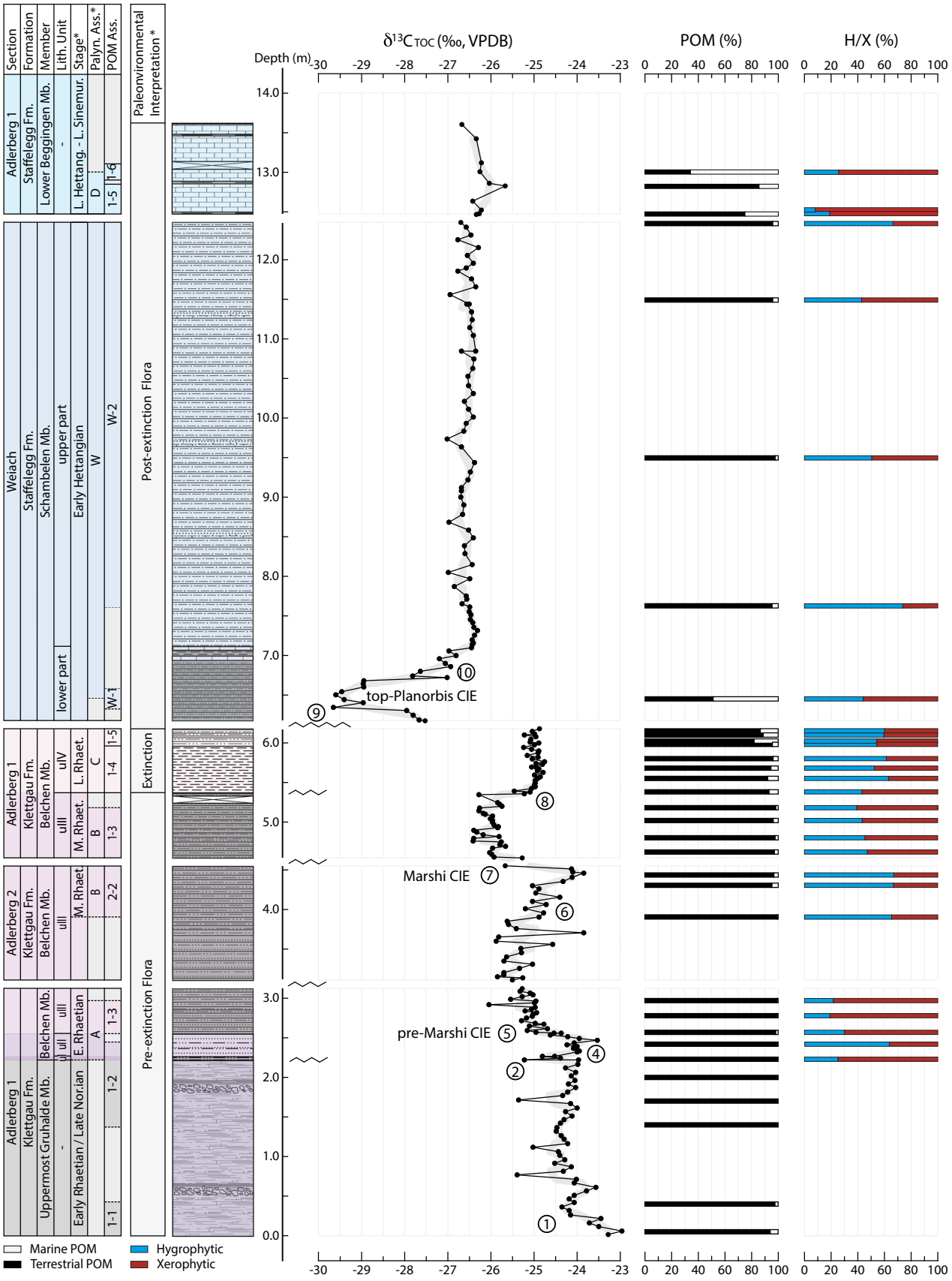
Section
Formation
Member
Lith. Unit
Stage*
Palyn. Ass.*
POM Ass.
Adlerberg 1
Staffelegg Fm.
Lower Beggingen Mb.
-
L. Hettang. - L. Sinemur.
D
1-5
1-6
Weiach
Staffelegg Fm.
Schambelen Mb.
lower part
upper part
Early Hettangian
W
W-1
W-2
Adlerberg 1
Klettgau Fm.
Belchen Mb.
ulll
ulV
M. Rhaet.
L. Rhaet.
B
C
1-3
1-4
1-5
Adlerberg 2
Klettgau Fm.
Belchen Mb.
ulll
M. Rhaet.
B
2-2
Adlerberg 1
Klettgau Fm.
Uppermost Gruhalde Mb.
Belchen Mb.
ulV
ulll
-
Early Rhaetian / Late Norian
E. Rhaetian
A
1-1
1-2
1-3
Paleoenvironmental Interpretation*
Post-extinction Flora
Extinction
Pre-extinction Flora
Depth (m)
δ13CTOC (‰, VPDB)
POM (%)
H/X (%)
top-Planorbis CIE
Marshi CIE
pre-Marshi CIE
Marine POM
Terrestrial POM
Hygrophytic
Xerophytic

◀**Fig. 5** Composite stratigraphic column of the Adlerberg 1, Adlerberg 2 and Weiach cores with $\delta^{13}C_{TOC}$, POM, and H/X data. Information about the palynological associations and stages and the paleoenvironmental interpretation are from Schneebeli-Hermann et al. (2018)

positive shift (**3**) within uI from lower and strongly fluctuating towards higher and more stable values is observed. An abrupt positive shift (**4**) is found between the top of uI and the lower part of uII (Fig. 2). This is followed by a gradual negative shift (**5**) of approx. − 1.5‰ within the upper part of uII (Figs. 2, 3). At Chilchzimmersattel, this negative shift also encompasses the lowermost part of uIII (online resource 2). This is followed by a continuous positive shift of + 2‰ (**6**) recorded within uIII in the Adlerberg 2 core and at Chilchzimmersattel (Fig. 3 and online resource 2). The abrupt negative shift (**7**) in the upper part of uIII is followed by a jump to higher values at the discontinuous contact between uIII and uIV (**8**, Figs. 2 and 3). In the Adlerberg cores, the following abrupt negative shift (**11**) of approx. − 1.5‰ (Figs. 2, 3) correlates with the erosive contact between uIV and the Beggingen Mb. Within the Schambelen Mb., a negative shift of more than − 2‰ is recorded in Weiach (**9**) followed by a positive shift (**10**) of + 3‰ in Weiach (Fig. 4) and + 2‰ in Frick (online resource 3). The uppermost shift (**12**) of + 2‰ is found within the Beggingen Mb. (online resource 3).

Carbon isotope measurements on isolated woody phytoclasts in the Adlerberg 1 core (Fig. 2) show a large scatter of up to 3.5‰ for different phytoclasts at the same depth. This large scatter is expected as carbon isotope values, even from the same plant, can vary by several per mill as shown by the scatter of 1.4‰ measured on four subsamples of a single woody phytoclast at a depth of 37.55 m (Fig. 2). Nevertheless, the $\delta^{13}C_{WP}$ record shows a negative shift of − 2.5‰ from the base to the top of uIII encompassing the two negative shifts (**5**) and (**6**) which is in good accordance with the $\delta^{13}C_{TOC}$ record showing a shift of − 2.4‰. Since translucent woody phytoclasts are potentially less oxidized than opaque woody phytoclasts, the two types were measured separately. However, no significant difference in their $\delta^{13}C$ values was observed.

6.2 OC/TN atomic ratios and nitrogen isotopes on total nitrogen

A total of eight intervals in the OC/TN (**a**–**g**) record and $\delta^{15}N_{TN}$ (**A**–**G**) can be correlated between the sections (Figs. 2, 3, 4, and online resources 1, 2, and 3) whereby the two records show clear anti-correlation between OC/TN and $\delta^{15}N_{TN}$. However, the OC/TN and $\delta^{15}N_{TN}$ records show differences in both magnitude of the shifts and absolute values at the different locations. The lowermost interval (**a/A**) encompasses the Gruhalde Mb. where OC/TN ratios are relatively constant around 3 and $\delta^{15}N_{TN}$ show values of about 3‰ with a more stable phase in the lower part and higher fluctuations in the upper part. Intervals (**b/B**) and (**d/D**) in uI and uIII are marked by increased OC/TN ratios of up to 30 and around 0.5‰ lighter $\delta^{15}N_{TN}$ values. In the intervals (**c/C**) and (**e/E**) in uII and uIV, OC/TN ratios decrease while $\delta^{15}N_{TN}$ remains around 3‰. In the interval (**f/F**) in the lower Schambelen Mb., the OC/TN ratios in Weiach and Frick are again up to 30 while only in Weiach a negative shift in $\delta^{15}N_{TN}$ of about – 1‰ is seen. The interval (**g/G**) within the upper part of the Schambelen Mb. is marked by constant OC/TN ratios around 10 and fluctuating $\delta^{15}N_{TN}$ values of around 2.5‰. The last interval (**h/H**) corresponds to the Beggingen Mb. and is characterized by increased OC/TN ratios and fluctuating somewhat lighter $\delta^{15}N_{TN}$ values.

6.3 POM and hygrophytic/xerophytic ratios

For the interpretation of the POM data, a terrestrial and a marine group of POM was established. The terrestrial particle group includes translucent and opaque wood, inertinite, cuticles, membranes, bisaccate pollen grains (including *Ovalipollis* spp.), Circumpolles, other pollen grains (including e.g. *Rhaetopollis germanicus* or *Perinopollenites elatoides*), spores, fungal remains, and *Chomotriletes* sp. The marine particle group includes amorphous organic matter (AOM), acritarchs, dinoflagellates, and foraminiferal test linings. Based on the relative abundances of these categories, different POM-associations were differentiated (Figs. 2, 3, 4, 6, and online resources 1 and 2).

Adlerberg 1 core: POM-association **1-1** (37.95–37.6 m) is dominated by woody phytoclasts (94%) with lots of translucent wood and only minor AOM (4%). POM-association **1-2** (36.60–35.58 m) is also dominated by woody phytoclasts (94%) but with increased opaque wood. Relative abundances of inertinite and sporomorphs are very low and marine particles were not encountered. POM-association **1-3** (35.43–34.27 m) is dominated by woody phytoclasts (90%) with high abundance of translucent wood particles and minor cuticle, circumpolles, and AOM (2%). POM-association **1-4** (34.07–33.47 m) is also dominated by woody phytoclasts (77%) but circumpolles, other pollen grains, and spores show markedly increased relative abundances. A contribution of marine OM is observed, as shown by AOM (4%), dinoflagellates (2%), and some acritarchs and foraminiferal test linings. POM-association **1-5** (33.43–32.90 m) is dominated by woody phytoclasts (71%). However, here the contribution of marine OM is higher as shown by increased AOM (15%) and the presence of acritarchs, dinoflagellates, and foraminiferal test linings. POM-association **1-6** (32.72 m) is rich in AOM

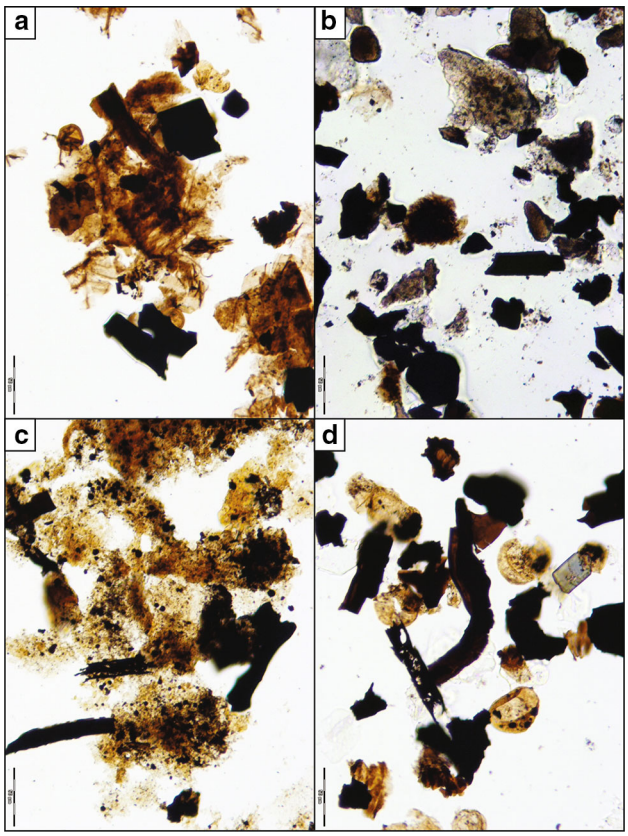

Fig. 6 POM associations. **a** POM-association 1-3 (Adlerberg 1 core, 35.43 m). **b** POM-association 1-4 (Adlerberg 1 core, 34.07 m). **c** POM-association W-1 (Weiach core, 704.24 m). **d** POM-association W-2 (Weiach core, 699.20 m). Scale bars represent 50 µm

(65%) while woody phytoclasts are subordinate (28%) and only few sporomorphs were encountered.

Adlerberg 2 core: POM-associations **2-1** and **2-2** are rather homogenous in the interval between 34.02 and 31.25 m with a dominance of woody particles (90%) and low sporomorph and marine particle contents. Only two samples (32.03 and 36.80 m) show increased sporomorph abundances (24 and 35%).

Adlerberg 3 core: POM-association **3-1** (35.25 and 34.25 m) shows abundant woody phytoclasts (51%) and sporomorphs (41%) while the marine fraction is low (4%).

Chilchzimmersattel outrcop: POM-association **C-1** (spanning uII and uIII) is characterized by woody phytoclasts (58%), sporomorphs (36%), and only minor marine contribution.

Weiach core: POM-association **W-1** (704.24 m) consists of AOM (49%), woody phytoclasts (43%), and palynomorphs. POM-association **W-2** (703.07–698.24 m) is dominated by woody particles (78%) while the marine contribution is very low.

Spore and pollen taxa were grouped into hygrophytic (plants adapted to humid conditions) and xerophytic (plants adapted to arid conditions) and variations in their relative abundance were determined by H/X ratios (Visscher and Van der Zwan 1981). Spores and few gymnosperm pollen taxa such as *Perinopollenites* spp. were classified as hygrophytic, whereas all other gymnosperm pollen as xerophytic. In the Adlerberg 1 core, the H/X ratios of the palynological association A are rather low. At the base of the palynological association B, the H/X ratios increase abruptly and then continuously further increase to the top of the palynological association C. Palynological association D shows again higher contributions of xerophytic elements. The H/X ratios of the palynological association W are similar to the ones in the palynological association C in the Adlerberg 1 core (Fig. 5).

7 Discussion

7.1 Evolution of the depositional environment from Late Triassic to Early Jurassic

The marls of the uppermost Gruhalde Mb. with dolomite layers and intraclasts are deposits of lacustrine to brackish mudflats, which were repeatedly flooded, fell dry, and were reworked. Fish scales, branchiopod crustaceans, and AOM indicate periods of water high-stand with an oxygenated sediment–water interface leading to low TOC contents. Periods with subaerial exposure are revealed by articulated skeletons of *Plateosaurus* in the clay pit of Frick (e.g. Sander 1992) and supported by bone fragments and an archosaur tooth found in the Adlerberg 2 core, which due to its size and good preservation suggests minimal transport, and by the occurrence of relatively large fragments of land plants.

The onset of an extensive marine transgression during Early and Middle Rhaetian caused a change from the continental mudflats to a high-energy marginal marine, current and storm-influenced depositional environment with strong terrestrial input from a river delta or an estuary (uI, uII, and lower part of uIII of the Belchen Mb.). This is documented by fine-grained sandstones with asymmetric current ripples showing unidirectional traction currents (presumably longshore currents or stream flow in the river mouth of a delta), a storm bed with abundant bivalve shells and reworked vertebrate remains at Chilchzimmersattel (Jordan et al. 2016), and a change in Sporomorph Ecogroups (SEGs) from lowland plant communities to a more coastal plant community (Schneebeli-Hermann et al. 2018). However, the source of OM remained entirely terrestrial (100% in uI and uII of the Adlerberg 1 core). The fining-upward sequence ranging from fine sandstones with current ripples and sandy siltstones in uI, uII, and the lower part of uIII to silty claystones in the upper part of uIII and

claystones in uIV documents the decreasing water energy due to the ongoing transgression. This is associated with a slight increase in marine OM input (3% in the upper part of uIII, 6% in the lower part of uIV, and 14% in the upper part of uIV of the Adlerberg 1 core). TOC contents reach their maximum values in the upper part of uIII while the terrestrial influence remains dominant with high proportion of terrestrial OM and quartz and mica observed throughout the Belchen Mb. This indicates that the supply of terrestrial OM and sediment persisted also during the following high sea level stand. Extensive bioturbation in uII suggests oxygenated bottom waters during the early stages of the transgression. The oxygenated bottom water conditions persisted for a longer time in the depositional area of Chilchzimmersattel, while in the Adlerberg area, anoxic bottom water conditions developed soon after. This is shown by the occurrence of bioturbation throughout uIII in the Chilchzimmersattel, while the Adlerberg 1 and 2 cores show a distinct lamination throughout uIII. The water depths remained shallow during the transgression and the entire coastal area was repeatedly subject to erosion, resulting in numerous presumably small sedimentary gaps indicated by discrete changes in lithology, TOC contents, OM compositions or abrupt changes in the isotopic composition within the Belchen Mb. Especially in the lower part of the Belchen Mb. these sedimentary gaps occur at different stratigraphic positions and often cannot directly be correlated between sections. Therefore, they can be regarded as local effects with a limited spatial extent showing the high influence of the bathymetry, river deltas or longshore currents on deposition. Due to these gaps, the sedimentary and isotope record of the Belchen Mb. is very variable even over short distances. Between late Middle Rhaetian and early Late Rhaetian, the high sea level stand was followed by a marine regression resulting in a gap between uIII and uIV, which can be observed in the Adlerberg 1 and 2 cores. This is documented by lag deposits enriched with bone fragments and teeth directly at the contact between uIII and uIV. The hiatus is further indicated by an abrupt change from palynological association B (Middle Rhaetian age) to association C (Late Rhaetian age, Schneebeli-Hermann et al. 2018) and by an abrupt positive $\delta^{13}C_{TOC}$ shift. During the deposition of uIV in Late Rhaetian, oxygenated bottom water conditions persisted for some time as indicated by low TOC contents and extensive bioturbation.

A major marine regression took place in northern Switzerland between the latest Rhaetian and earliest Hettangian and caused a substantial sedimentary hiatus so that the uppermost Rhaetian and lowermost Hettangian sediments are not preserved (Schneebeli-Hermann et al. 2018). This major marine regression influenced the Adlerberg and Chilchzimmersattel areas during a different time period than the Frick and Weiach areas (Fig. 1). In the Adlerberg and Chilchzimmersattel areas, it caused either non-deposition and/or erosion between latest Rhaetian and Late Hettangian resulting in the preservation of the lower to upper Rhaetian sediments of the Belchen Mb. and in the absence of the uppermost Rhaetian and lower Hettangian sediments of the Schambelen Mb. In the Chilchzimmersattel area, where uIV is missing, this marine regression was seemingly more effective than in the Adlerberg area, where uIV is preserved. In contrast, in the region around Frick and Weiach, the marine regression either started earlier or the erosion was more effective but already ended in Early Hettangian so that the Rhaetian sediments of the Belchen Mb. are absent while the Hettangian sediments of the Schambelen Mb. containing the palynological association W are preserved. An earlier onset of sedimentation after the marine regression in Weiach compared to Frick and ultimately the Adlerberg and Chilchzimmersattel is also indicated by the wedging-out of the Schambelen Mb. towards the west (Reisdorf et al. 2011) and by the fact that in Weiach the negative shift in the lower part (**9**) is recorded, while in Frick this is not the case (Fig. 4 and online resource 3).

Deposition of the Schambelen Mb. took place in Early Hettangian (upper Planorbis and Liasicus zones) in a marine environment as documented by the common occurrence of ammonites and echinoderms while proximity to land is indicated by insect remains (Heer 1865; Etter 2016), mica, and quartz. Despite the occurrence of marine biota like ammonites and echinoderms, POM analysis show a distinctly higher proportion of marine OM (49%) only in the lower part of the Schambelen Mb. while the upper part is again strongly dominated by terrestrial OM (96%). During deposition of the lower part of the Schambelen Mb., oxygen concentrations in the bottom water were low (Schwab and Spangenberg 2007; Etter 2016) resulting in enhanced OM preservation.

The Beggingen Mb. was deposited in a marine environment with normal salinity as indicated by the rich marine fauna. However, especially for the lowermost part of the Beggingen Mb., proximity to land is evident since the terrestrial OM fraction is high. During the deposition of the basal Beggingen Mb., strong water energy prevailed as indicated by the bioclastic grainstones with iron ooids and disarticulated valves of the bivalve *Cardinia* sp. in stable convex-up position. The influence of water energy decreased soon afterward, as documented by the micritic matrix as well as by the occurrence of the bivalve *Gryphaea arcuata* in life position and a bivalve *Cardinia* sp. with articulated valves in butterfly preservation. The frequent occurrence of phosphorite nodules suggest repetitive development of hardground conditions with exposure of the seafloor to currents.

7.2 Carbon/nitrogen atomic ratios and nitrogen isotopes

Aquatic OM generally shows low C/N ratios of 6.6 (e.g. Redfield 1934), while vascular land plants have C/N ratios ≥ 20 (e.g. Meyers 1994) due to their high cellulose content. Therefore, changes in C/N ratios of OM can be used to detect changes in terrestrial (vascular) and marine (aquatic) OM contributions. Modern terrestrial OM is generally characterized by low $\delta^{15}N$ values of around 1‰, while aquatic OM shows significantly higher $\delta^{15}N$ values of around 7.5‰ (Ogrinc et al. 2005 and references therein). Hence, changes in relative proportion of aquatic and terrestrial OM potentially results in variations in the $\delta^{15}N$ record. However, C/N ratios and $\delta^{15}N$ in sediments can also be influenced by inorganic nitrogen in the form of soil-derived ammonium (Scheffer and Schachtschabel 1984). Due to this inorganic nitrogen, C/N ratios of sediments containing additional inorganic nitrogen will decrease and $\delta^{15}N$ values will be closer to the atmospheric $\delta^{15}N$ composition of 0‰ than pure OM (Schubert and Calvert 2001). Here, C/N ratios of sediments containing both organic and inorganic nitrogen were measured and therefore C/N ratios are referred to as organic carbon/total nitrogen (OC/TN) and $\delta^{15}N$ as $\delta^{15}N_{TN}$.

The relation between TN and TOC contents (Fig. 7) is described by $TN = 3.13 \times OC\ E\text{-}02 + 5.17\ E\text{-}02$ and shows a strong correlation ($R^2 = 0.95$, n = 89) for the Adlerberg 1 and Weiach cores containing all of the analyzed lithologies. While the high R^2 indicates that OM is the main control on TN and OC/TN ratios in the sediment, the positive Y intercept indicates the presence of inorganic nitrogen in at least some of the samples. This influence of inorganic nitrogen is particularly important in sediments with low OM contents. Therefore, only in the OM-rich lithologies, such as uI and uIII of the Belchen Mb. and the lower part of the Schambelen Mb., do the OC/TN and $\delta^{15}N_{TN}$ reflect the composition of OM. High OC/TN ratios observed in uI and uIII of the Belchen Mb. fit well with the POM data suggesting a predominately terrestrial source of OM. In the lower part of the Schambelen Mb., however, OC/TN ratios with values of up to 30 contradict the POM data suggesting 49% marine OM. A possible explanation for this is that C/N and $\delta^{15}N$ of OM can undergo alteration during burial and early diagenesis (e.g. Lehmann et al. 2002; Robinson et al. 2012) with differences in oxygen exposure likely being the dominant control on alteration. Since framboidal pyrite occurs in all of the OM-rich intervals, euxinic porewater conditions are evident. In the case of the Schambelen Mb., euxinic conditions even extended into the photic zone as revealed by biomarker evidence (Schwab and Spangenberg 2007). Under such conditions, degradation of OM can lead to a depletion in $\delta^{15}N$ while the C/N ratios remain constant (Lehmann et al. 2002). Since the OM in in the lower part of the Schambelen Mb. consists of a mixture of easily degradable nitrogen-rich AOM and more resistant nitrogen-poor terrestrial OM, a preferential degradation and stronger alteration of AOM compared to the terrestrial OM is likely (Meyers 1994). A stronger alteration of the marine fraction of OM also could explain the more depleted $\delta^{15}N_{TN}$ in the lower part of the Schambelen Mb. compared to the Belchen Mb.

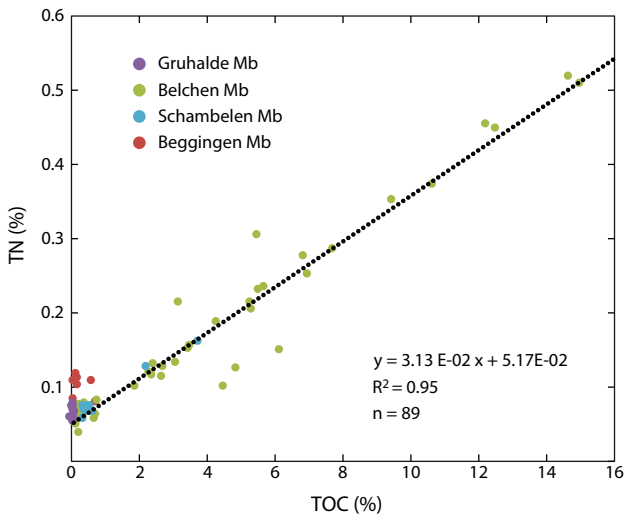

Fig. 7 Correlation between TOC and TN contents for the Adlerberg 1 and Weiach cores

7.3 Carbon isotope stratigraphy and comparison with other carbon isotope records across the Triassic–Jurassic boundary

POM analyses show a predominance of terrestrial OM in almost all sediments. In the stratigraphic interval where the negative shifts (**1**), (**2**), (**5**), and (**7**) occur, the terrestrial OM comprises 96–100% of the total OM. Therefore, all these carbon isotope shifts do not reflect variable mixing of terrestrial and marine OM but represent primary changes in the carbon cycle. Shifts due to changes of the relative proportions of different types of terrestrial OM including wood particles, pollen, and spores can also be excluded. Evidence for this is the $\delta^{13}C_{WP}$ record showing the same shifts as the $\delta^{13}C_{TOC}$ record and the POM-associations **1-1**, **1-2**, **1-3**, and **2-2** showing average proportions of pollen and spores always below 8% while the proportion of wood particles is never smaller than 84%. Furthermore, a shift due to mixing of translucent and opaque wood particles with different proportions can be excluded because no significant systematic differences between the two types of wood particles was observed. Consequently, the observed negative shifts in $\delta^{13}C_{TOC}$ of the Gruhalde and Belchen

Mbs. reflect global changes in the carbon cycle and can be used for the correlation with other sections. However, the presence of sedimentary gaps has to be taken into account when interpreting and correlating the fragmentary isotope record of the studied sections. This applies in particular to the shifts (**2**), (**7**), (**8**), and (**11**).

The negative shift (**7**), which is recorded in the Adlerberg 1 and 2 cores and in the Chilchzimmersattel outcrop, occurs in the upper part of uIII of the Belchen Mb. with the palynological association B and shows the peak with the most negative $\delta^{13}C$ values directly at the contact to the following uIV of the Belchen Mb. with palynological association C. Based on the palynological correlation to the Kuhjoch section in Austria by Schneebeli-Hermann et al. (2018), the negative shift (**7**) is identified as the Marshi CIE (Fig. 8) which takes place directly before the global extinction interval (Lindström et al. 2017). In our sections, the Marshi CIE has an amplitude of approx. − 2.5‰ (Fig. 5), considerably smaller than the almost − 6‰ in the Kuhjoch section (Ruhl et al. 2009) but similar to the shift of − 2.3‰ in St. Audrie's Bay, southwest England

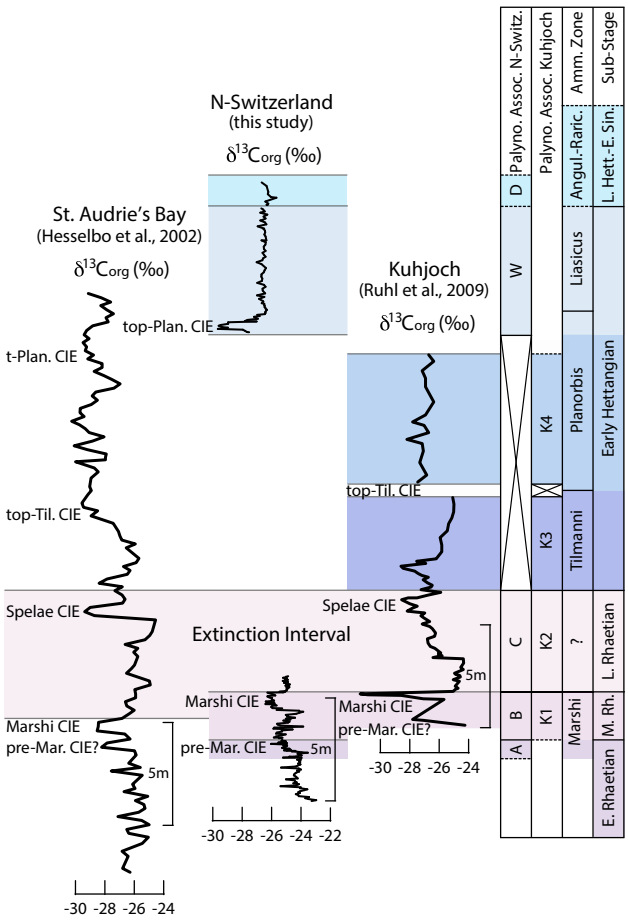

Fig. 8 Correlation of the $\delta^{13}C_{TOC}$ record of northern Switzerland to the Kuhjoch section (Tethys) and the St. Audrie's Bay section (CEB). Modified from Lindström et al. (2017)

(Hesselbo et al. 2002). However, since there is evidence for a hiatus at the contact between uIII and uIV as well as presumably reworked wood fragments in the lowermost part of uIV showing $\delta^{13}C_{WP}$ values of about − 30‰ we suggest that only the lower part of the Marshi CIE is preserved in the studied sections. Directly below the Marshi CIE the negative shift (**5**) of approx. − 2‰ in the $\delta^{13}C_{TOC}$ record is found within uII and in the lower part of uIII of the Belchen Mb. with the palynological association A. Although a palynological correlation to the Kuhjoch section is not possible (Schneebeli-Hermann et al. 2018) a correlation of this negative shift to other sections is possible based on its stratigraphic position as the last negative shift prior to the Marshi CIE (Fig. 8). This shift is here termed pre-Marshi CIE. The Spelae CIE in the uppermost part the global extinction interval during latest Rhaetian as well as the top-Tilmanni CIE during the earliest Jurassic (Lindström et al. 2017) are absent in the studied sections because of a major sedimentary gap (Fig. 8). Evidence for the lack of the Spelae CIE is the thickness of uIV with the palynological association C of only 0.8 m in the Adlerberg 1 core and 0.4 m in the Adlerberg 2 core while this interval in the Kuhjoch and St. Audrie's Bay sections is around 6 m thick. Further evidence is provided by the constant and less negative isotope values within uIV that in the Kuhjoch and St. Audrie's Bay sections occur between the Marshi and Spelae CIEs. The earliest Hettangian sediments containing the Tilmanni zone and the lower part of the Planorbis zone are also not preserved in the studied sections as shown by the absence of a palynological association corresponding to the palynozone K3 from the Kuhjoch section (Schneebeli-Hermann et al. 2018) and by the ammonites found in the lower part of the Schambelen Mb. belonging to the upper Planorbis zone (Reisdorf et al. 2011). Being located in the upper Planorbis zone, the negative shift (**9**) of − 2.1‰ within the lower part of the Schambelen Mb. in Weiach can be correlated with a negative shift of approx. − 2.5‰ occurring in the top of the Planorbis zone of the St. Audrie's Bay section (Hesselbo et al. 2002). This shift is here termed top-Planorbis CIE. It cannot be observed in the Kuhjoch section since no $\delta^{13}C$ measurements are available for the uppermost part of the Planorbis zone (Fig. 8). The top-Planorbis CIE (**9**) as well as the subsequent positive shift (**10**) coincide with distinct changes in the source of OM from 51% terrestrial in the middle of the lower part of the Schambelen Mb. to around 96% terrestrial again in the upper part of the Schambelen Mb. (Fig. 5). Therefore, the top-Planorbis CIE with an amplitude of − 2.1‰ and the subsequent positive shift with an amplitude of approx. + 3‰ might be influenced by the change in OM source. For the $\delta^{13}C$ values at the base of the Schambelen Mb. prior to the top-Planorbis CIE, no POM data are available to show if there is a change in

source of OM between the base and the top of the top-Planorbis CIE. However, the lower part of the Schambelen Mb. is very homogeneous and since major changes in OM are bound to changes in the depositional environment and sediment type, a major change in the source of OM within the lower part of the Schambelen Mb. is unlikely. Also, even if assuming 100% terrestrial OM for the base of the Schambelen Mb., the top-Planorbis CIE cannot be solely explained by a 50% change to more marine OM because of the similar $\delta^{13}C$ signature (within 2‰) of the two sources in Early Jurassic. The same holds for the subsequent positive shift (**10**) after the top-Planorbis CIE (Fig. 8). We conclude that both the top-Planorbis CIE and the subsequent positive shift reflect a global change in the carbon cycle and are only to some degree influenced by a change in OM. The positive shift (**10**) is associated on a regional scale with concurrent changes from bituminous shales to low-TOC claystones and records the recovery of the carbon cycle after the top-Planorbis CIE.

7.4 Climatic impacts of enhanced atmospheric CO_2 concentrations: Changes in terrestrial vegetation and development of marine anoxia

Changes in the relative proportion of xerophytic and hygrophytic plants are indicative for changes in humidity. Rather low H/X ratios of the palynological association A indicate relatively dry conditions during Early Rhaetian (Fig. 5). Climatic conditions changed towards more humid during Middle Rhaetian as indicated by the increase of the H/X ratios from palynological association A to B. The following continuous increase of the H/X ratios from the base of association B to the top of association C shows that the humid conditions intensified from Middle to Late Rhaetian. Similar humidity also prevailed during Early to Late Hettangian as documented by the high H/X ratios in the association W. The association D with higher contributions of xerophytic elements indicates a return to dryer climatic conditions during Late Hettangian and Early Sinemurian. The onsets of intervals with enhanced humidity correlate with carbon cycle perturbations in the upper part of the pre-Marshi-CIE, Marshi-CIE, and top-Planorbis CIE. The onsets of enhanced humidity contemporaneous with isotopically light $\delta^{13}C$ values can be interpreted as result of increased atmospheric CO_2 concentrations leading to intensification of the hydrological cycle. These humid climate conditions prevailed also in times of recovery of the global carbon cycle subsequent to the CIEs as in uIV of the Belchen Mb. and the upper part of the Schambelen Mb. The climatic conditions between latest Rhaetian and earliest Hettangian, however, are not recorded in the studied sections.

Contemporaneous with the negative CIEs and humid climatic conditions during Middle Rhaetian as well as later in Early Hettangian times, oxygen depleted bottom water conditions developed in northern Switzerland as shown by a lack of bioturbation and enhanced OM preservation leading to high TOC contents of up to 15%. The co-occurrence of increased TOC contents and/or laminated shales and negative CIEs was also observed in other locations in both the CEB (e.g. Hesselbo et al. 2004; Črne et al. 2011; Lindström et al. 2012) and in the Tethyan realm (e.g. Galli et al. 2005; Ruhl et al. 2009; Bonis et al. 2010; Felber et al. 2015). The wide geographic distribution and the occurrence of the oxygen depleted bottom waters across ocean basins demonstrates that this was not a local phenomenon but a climate-driven event as proposed by Bonis et al. (2010).

8 Conclusions

As a result of an extensive marine transgression, the depositional environment of northern Switzerland underwent a change from lacustrine to brackish mudflats during Late Norian or Early Rhaetian toward a marginal marine depositional environment with influence of estuaries or river deltas and a predominant terrestrial source of OM during Rhaetian. During Hettangian, a marine depositional environment with a marine fauna evolved. However, the source of OM remained predominantly terrestrial and only in the lowermost Jurassic sediments and in the uppermost part of the studied sections the contribution of marine OM exceeded 25%. Due to the shallow water environment, the sedimentary record contains several gaps and shows strong lateral variations even over short distances. Besides several locally occurring small sedimentary gaps between Early and Late Rhaetian, a major marine regression took place between latest Rhaetian and Early Hettangian and influenced the Adlerberg and Chilchzimmersattel areas during a different time period than the Frick and Weiach areas. In both cases, the uppermost Rhaetian and the lowermost Hettangian sediments are missing. Several negative carbon isotope excursions recording perturbations of the global carbon cycle are preserved in northern Switzerland which based on palynology, ammonite zonation, and their stratigraphic position are here correlated to sections in the CEB and Tethys realms. Correlated negative shifts in the $\delta^{13}C$ record include the Marshi CIE with an amplitude of approx. − 2.5‰ in the upper part of uIII of the Belchen Mb., the here newly defined top-Planorbis CIE with an amplitude of − 2.1‰, and the here newly defined pre-Marshi CIE in the upper part of uII and in the lower part of uIII of the Belchen Mb. Between Early and Middle Rhaetian, the climate shifted from arid to more humid

conditions. Humid conditions intensified in Late Rhaetian and also persisted during Hettangian until in the Early Sinemurian more arid conditions developed. The onsets of these intervals with enhanced humidity correlate with the upper part of the pre-Marshi-CIE, the Marshi-CIE, and the top-Planorbis CIE. This suggests that the humid conditions were triggered by increased atmospheric CO_2. Contemporaneous with the negative CIEs and more humid climate conditions, wide-spread marine anoxia developed during Middle Rhaetian and lasted until or evolved again in Early Hettangian.

While POM analyses are a reliable tool for detecting changes in the proportions of terrestrial and marine OM in the sedimentary record, OC/TN ratios and $\delta^{15}N_{TN}$ in this marginal marine setting are strongly influenced by changes in lithology, OM content, and degradation and have to be interpreted with caution if they are not combined with POM analyses for validation. Multiple locations were studied in order to obtain a record as continuous as possible using a combination of POM data, OC/TN, $\delta^{15}N_{TN}$, $\delta^{13}C_{TOC}$, and $\delta^{13}C_{WP}$ for disentangling changes in the source of OM from changes in the global carbon cycle. This record shows that the Triassic–Jurassic carbon cycle perturbations were sufficiently pronounced to be recorded in a shallow marginal sea system with only minor overprint from mixing between terrestrial and marine OM inputs.

Acknowledgements We would like to thank Stewart Bishop and Madalina Jaggi for assistance in the laboratory and Stefan Wohlwend as well as André Strasser and an anonymous reviewer for their suggestions to improve this manuscript. We would also like to thank the University of Basel and the national cooperative for the disposal of radioactive waste of Switzerland (NAGRA) for access to core material.

References

Arthur, M. A., Dean, W. E., & Claypool, G. E. (1985). Anomalous enrichment in modern marine organic carbon. *Nature, 315,* 216–218.

Bacon, K. L., Belcher, C. M., Hesselbo, S. P., & McElwain, J. C. (2011). The Triassic–Jurassic boundary carbon isotope excursions expressed in taxonomically identified leaf cuticles. *Palaios, 26,* 461–469.

Bartolini, A., Guex, J., Spangenberg, J. E., Schoene, B., Taylor, D. G., Schaltegger, U., et al. (2012). Disentangling the Hettangian carbon isotope record: implications for the aftermath of the end-Triassic mass extinction. *Geochemistry, Geophysics, Geosystems, 13,* 1–11.

Beerling, D. J., & Berner, R. A. (2002). Biogeochemical constraints on the Triassic–Jurassic boundary carbon cycle event. *Global Biogeochemical Cycles, 16,* 3.

Bonis, N. R., Ruhl, M., & Kürschner, W. M. (2010). Climate change driven black shale deposition during the end-Triassic in the western Tethys. *Palaeogeography, Palaeoclimatology, Palaeoecology, 290,* 151–159.

Cifuentes, L. A., Coffins, R. B., Slolrzano, L., Cardenas, W., Espinoza, J., & Teilley, R. R. (1996). Isotopic and elemental variations of carbon and nitrogen in a mangrove estuary. *Estuarine, Coastal and Shelf Science, 43,* 781–800.

Črne, A. E., Weissert, H., Gorican, S., & Bernasconi, S. M. (2011). A biocalcification crisis at the Triassic–Jurassic boundary recorded in the Budva Basin (Dinarides, Montenegro). *Geological Society of America Bulletin, 123,* 40–50.

Etter, W. (2016) Palaeoecology of the lower Jurassic Schambelen member of northern Switzerland. Swiss Geoscience Meeting, abstract volume, pp 144–145.

Felber, R., Weissert, H. J., Furrer, H., & Bontognali, T. R. R. (2015). The Triassic–Jurassic boundary in the shallow-water marine carbonates from the western Northern Calcareous Alps (Austria). *Swiss Journal of Geosciences, 108,* 213–224.

Fischer, J., Voigt, S., Franz, M., Schneider, J., Joachimski, M., Tichomirowa, M., et al. (2012). Palaeoenvironments of the late Triassic Rhaetian Sea: Implications from oxygen and strontium isotopes of hybodont shark teeth. *Palaeogeography, Palaeoclimatology, Palaeoecology, 353–355,* 60–72.

Galli, M. T., Jadoul, F., Bernasconi, S. M., & Weissert, H. (2005). Anomalies in global carbon cycling and extinction at the Triassic/Jurassic boundary: evidence from a marine C-isotope record. *Palaeogeography, Palaeoclimatology, Palaeoecology, 216,* 203–214.

Guex, J., Bartolini, A., Atudorei, V., & Taylor, D. (2004). High-resolution ammonite and carbon isotope stratigraphy across the Triassic–Jurassic boundary at New York Canyon (Nevada). *Earth and Planetary Science Letters, 225,* 29–41.

Hallam, A. (2001). A review of the broad pattern of Jurassic sea-level changes and their possible causes in the light of current knowledge. *Palaeogeography, Palaeoclimatology, Palaeoecology, 167,* 23–37.

Hayes, J. M., Strauss, H., & Kaufman, A. J. (1999). The abundance of ^{13}C in marine organic matter and isotopic fractionation in the global biogeochemical cycle of carbon during the past 800 Ma. *Chemical Geology, 161,* 103–125.

Heer, O. (1865). *Die Urwelt der Schweiz*. Zürich: Schulthess.

Hesselbo, S. P., Robinson, S. A., & Surlyk, F. (2004). Sea-level change and facies development across potential Triassic–Jurassic boundary horizons, SW Britain. *Journal of the Geological Society, London, 161,* 365–379.

Hesselbo, S. P., Robinson, S. A., Surlyk, F., & Piasecki, S. (2002). Terrestrial and marine extinction at the Triassic–Jurassic boundary synchronized with major carbon-cycle perturbation: a link to initiation of massive volcanism? *Geology, 30,* 251–254.

Jordan, P. (1983). Zur Stratigraphie des Lias zwischen Unterem Hauenstein und Schinznach (Solothurner und Aargauer Faltenjura). *Eclogae Geologicae Helvetiae, 76,* 355–379.

Jordan, P., Pietsch, J. S., Bläsi, H., Furrer, H., Kündig, N., Looser, N., et al. (2016). The middle to late Triassic Bänkerjoch and Klettgau formations of northern Switzerland. *Swiss Journal of Geoscience, 109*(2), 257–284.

Killops, S., Killops, V. (2005). Introduction to organic geochemistry, 2nd edition. Oxford: Blackwell Publishing.

Kump, L. R., & Arthur, M. A. (1999). Interpreting carbon-isotope excursions: Carbonates and organic matter. *Chemical Geology, 161,* 181–198.

Lauber, L. (1991). Bahn 2000, Abschnitt Muttenz—Sissach, Los 1.2, Adlertunnel (Bauprojekt), Geologischer Bericht. Geologisches Institut, Universität Basel, Basel.

Lehmann, M. F., Bernasconi, S. M., Barbieri, A., & McKenzie, J. A. (2002). Preservation of organic matter and alteration of its carbon and nitrogen isotope composition during simulated and in situ early sedimentary diagenesis. *Geochimica et Cosmochimica Acta, 66,* 3573–3584.

Lindström, S., van de Schootbrugge, B., Dybkjær, K., Pedersen, G. K., Fiebig, J., Nielsen, L. H., et al. (2012). No causal link between terrestrial ecosystem change and methane release during the end-Triassic mass-extinction. *Geology, 40,* 531–534.

Lindström, S., van de Schootbrugge, B., Hansen, K. H., Pedersen, G. K., Alsen, P., Thibault, N., et al. (2017). A new correlation of Triassic–Jurassic boundary successions in NW Europe, Nevada and Peru, and the Central Atlantik Magmatic Province: A timeline for the end-Triassic mass extinction. *Palaeogeography, Palaeoclimatology, Palaeoecology, 478,* 80–102.

Matter, A., Peters, T., Bläsi, H. R., Meyer, J., Ischi, H., & Meyer, C. (1988). Sondierbohrung Weiach Untersuchungsbericht (Gemeinde Weiach, Kanton Zürich, Schweiz), Textband. Nagra Technischer Bericht, NTB 88-08. *Beiträge zur Geologie der Schweiz, Geotechnische Serie, 73,* 1–183.

McElwain, J. C., Wagner, P. J., & Hesselbo, S. P. (2009). Fossil plant relative abundances indicate sudden loss of Late Triassic biodiversity in East Greanland. *Science, 324,* 1554–1556.

Meyers, P. A. (1994). Preservation of elemental and isotopic source identification of sedimentary organic matter. *Chemical Geology, 114,* 289–302.

Ogrinc, N., Fontolan, G., Faganeli, J., & Covelli, S. (2005). Carbon and nitrogen isotope compositions of organic matter in coastal marine sediments (the Gulf of Trieste, N Adriatic Sea): indicators of sources and preservation. *Marine Chemistry, 95,* 163–181.

Pálfy, J., Demény, A., Haas, J., Hetényi, M., Orchard, M. J., & Vetö, I. (2001). Carbon isotope anomaly and other geochemical changes at the Triassic–Jurassic boundary from a marine section in Hungary. *Geology, 29,* 1047–1050.

Redfield, A. (1934). On the proportions of organic derivatives in sea water and their relation to the composition of plankton. In Daniel, R.J. (ed James Johnstone Memorial Volume), University Press of Liverpool, pp 177–192.

Reisdorf, A. G., Wetzel, A., Schlatter, R., & Jordan, P. (2011). The Staffelegg Formation: a new stratigraphic scheme for the Early Jurassic of northern Switzerland. *Swiss Journal of Geosciences, 104,* 97–146.

Robinson, R. S., Kienast, M., Luiza Albuquerque, A. L., Altabet, M., Contreras, S., De Pol Holz, R., et al. (2012). A review of nitrogen isotopic alteration in marine sediments. *Paleoceanography, 27,* PA4203.

Ruhl, M., Kürschner, W. M., & Krystyn, L. (2009). Triassic–Jurassic organic carbon isotope stratigraphy of key sections in the western Tethys realm (Austria). *Earth and Planetary Science Letters, 281,* 169–187.

Sander, P. M. (1992). The Norian *Plateosaurus* bonebeds of central Europe and their taphonomy. *Palaeogeography, Palaeoclimatology, Palaeoecology, 93,* 255–299.

Scheffer, F., &Schachtschabel, P. (1984). *Lehrbuch der Bodenkunde*. Stuttgart: Enke Verlag.

Schneebeli-Hermann, E., Looser, N., Hochuli, P. A., Furrer, H., Reisdorf, A. G., Wetzel, A., et al. (2018). Palynology of Triassic–Jurassic boundary sections in Northern Switzerland. *Swiss Journal of Geosciences, 111,* 99–115.

Schubert, C. J., & Calvert, S. E. (2001). Nitrogen and carbon isotopic composition of marine and terrestrial organic matter in Arctic Ocean sediments: implications for nutrient utilization and organic matter composition. *Deep-Sea Research I, 48,* 789–810.

Schwab, V. F., & Spangenberg, J. E. (2007). Molecular and isotopic characterization of biomarkers in the Frick Swiss Jura sediments: A palaeoenvironmental reconstruction on the northern Tethys margin. *Organic Geochemistry, 38,* 419–439.

Sepkoski, J. J. (1996). Patterns of the Phanerozoic extinction: A perspective from global data bases. In O. H. Walliser (Ed.), *Global events and event stratigraphy in the Phanerozoic* (pp. 35–51). Berlin: Springer.

Stampfli, G. M., Kozur, H. W. (2006). Europe from the Variscan to the Alpine cycles. Gee, D.G., Stephenson, R.A. (Eds.), European lithosphere dynamics. Geological Society Memoir 32, pp. 333–343.

Traverse, A. (2007). *Paleopalynology*. Dordrecht: Springer.

Visscher, H., & Van Der Zwan, W. A. (1981). Palynology of the circum-Mediterranean Triassic: phytogeographical and palaeoclimatological implications. *Geologische Rundschau, 70,* 625–636.

Ziegler, P. A. (1990). *Geological Atlas of Western and Central Europe. Shell Internationale Petroleum Maatschappij B.V* (2nd ed.). Bath: Geological Society Publishing House.